0.2M-$(NH_4)_2HPO_4$ and 0.01M $NbCl_5$ solutions were mixed and stirred with a magnetic bar. The Nb/(Nb+P) molar ratio of the mixing solution was set to 0.0000, 0.0167 and 0.1667. The pH of the mixing solution was adjusted to 10 using 1N-NaOH. 0.2M-$Ca(NO_3)_2$ was slowly dropped in the mixing solution (20ml/min) The ionic content of those starting solutions are shown in table 1. The pH was monitored and the reaction was terminated at pH 10.0. After the reaction, the suspension was stirred for 24h at room temperature. The precipitates were centrifuged at 3000rpm for 5min and washed with distilled water. The obtained apatites were annealed at 800°C for 2h (heating rate: 5°C/min). In this study, those precipitates obtained by reaction of $Ca(NO_3)_2$ solution and the mixing solution with different Nb/(Nb+P) molar ratio of 0.000, 0.0167 and 0.1667 are named HAp , NbHAp-I and NbHAp-II, respectively.

Characterization of NbHAp

The NbHAps were characterized by X-ray diffraction analysis (XRD, Rigaku, Rint2000). Ca, P and Nb ions concentrations in apatites are measured by inductively coupled plasma (ICP, Hewlett-Packard, HP4500). Microstructural evaluation was performed by scanning electron microscopy (SEM) and energy dispersive X-ray spectroscopy (EDS) (JEOL, LV5800). The chemical state of Nb ions in HAp was investigated by X-ray photon spectroscopy (XPS, Shimadzu, ESCA-3200).

Osteogenesis evaluation of NHOst cultured with NbHAp

NHOst were purchased from BioWhittaker Inc.(Walkersville,MD). The NHOst were maintained in alpha minimum essential medium (αMEM, Gibco, Grand Island, NY) containing 10%-FCS in incubators at 37°C in a humidified atmosphere with 5% CO_2. All assays were performed using αMEM containing 10%-FCS supplemented with 10mM beta-glycerophosphate. NHOst cells (4×10^4 cells/well/ml) were co-cultured with 5mg of the apatites for 7days to evaluated the effects of the apatites on NHOst.

Proliferation of NHOst cells cultured with the apatites was estimated by Tetracolor One assay (Seikagaku Co., Ltd. Tokyo, Japan), which incorporates an oxidation reduction indicator based on detection of metabolic activity. After 7-days incubation, 2%-TetraColor One/αMEM solution was added to each well, followed by 2h incubation. The absorbance of the supernatant at 450nm was estimated using μQuant spectrophotometer (Bio-tek Instrument, Inc., Winooski, VT). After estimating the proliferation, the cells were washed by phosphate–buffered saline (PBS(-)), followed by addition of 1ml of 0.1M glycine buffer (pH=10.5) containing 10mM $MgCl_2$, 0.1mM $ZnCl_2$ and 4mM p-nitrophenylphosphate sodium salt. After incubating at room temperature for 5min, the absorbance at 405 nm was detected using the μQuant spectrophotometer to evaluated alkaline phosphatase (ALP) activity of the test cells.

Results and Discussion

XRD patterns of NbHAps prepared by wet chemical process are shown in Fig.1(a). Irrespective of Nb/(Nb+P) molar ratio in starting solution, the precipitates were identified as monolithic HAp.

Table1. The ionic content of starting solution and the composition of the obtained precipitates.

Samples	Ionic content of Starting Solution*,			Theoretical Ca/(Nb+P)**	Nb/(Nb+P)**		Color of Precipitates
	Ca	PO_4	Nb		Theoretical	Measured**	
HAp	60.0	36.0	0.0	1.67	0.0000	-	White
NbHAp-I	60.0	35.4	0.6	1.67	0.0167	0.015	Pale yellow
NbHAp-II	60.0	30.0	6.0	1.67	0.1667	0.082	Buff yellow

*mmol, **Molar ratio, ***The precipitates were dissolved with HCl and the ionic concentration of HCl solutions were measured by ICP.

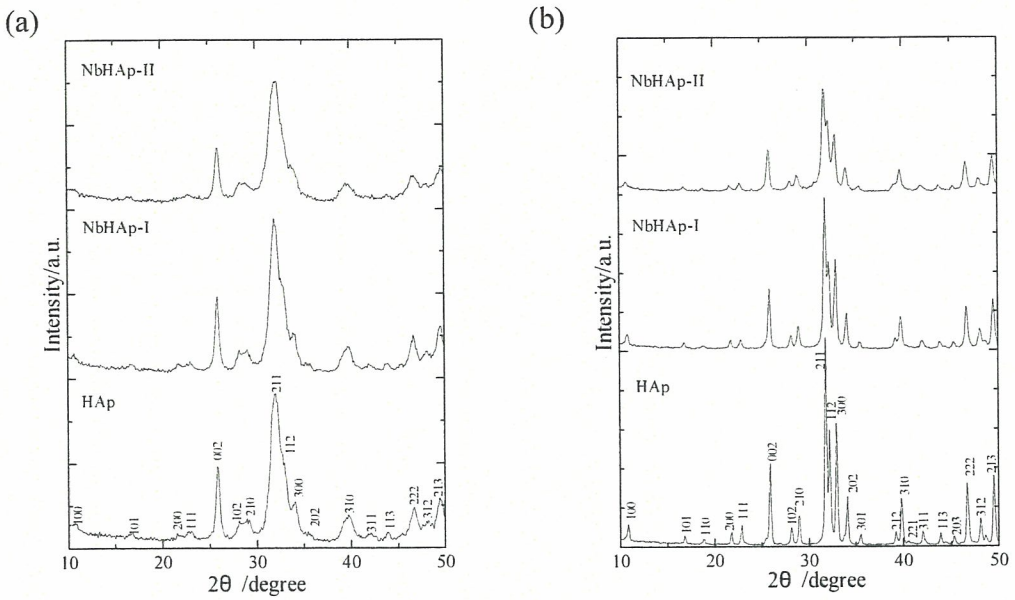

Fig.1. XRD patterns of HAp and NbHAp-I and NbHAp-II before (a) and after (b) annealing(800°C, 2h).

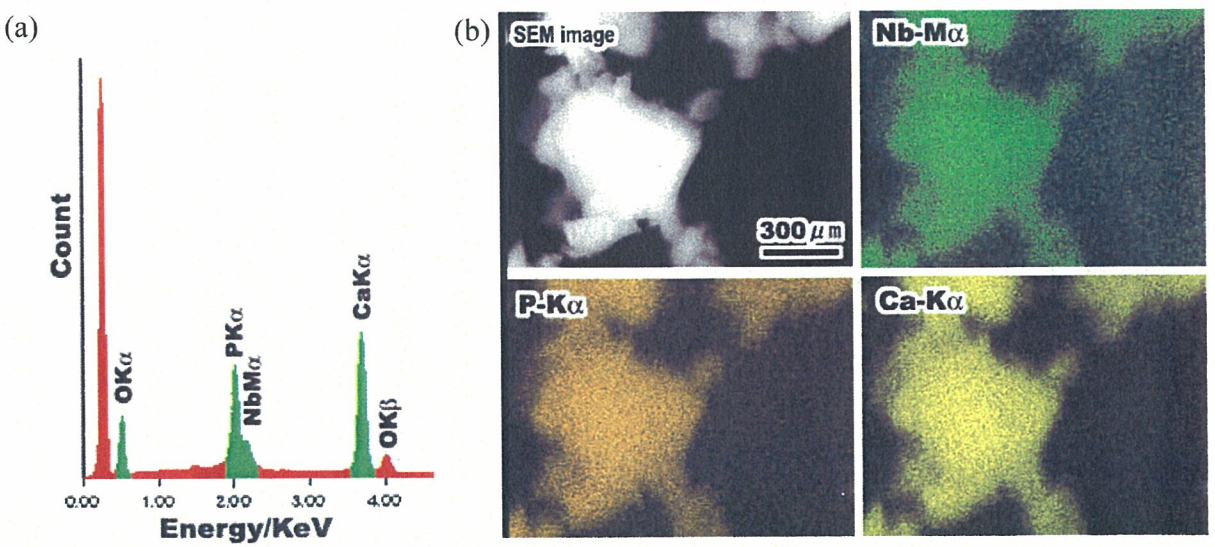

Fig.2. SEM-EDX analysis of NbHAp-II. ((a) An EDX spectrum and (b) SEM image and element mapping images of Nb, Ca and P).

As shown in Table1, the Nb/(Nb+P) molar ratio of NbHAp-I and NbHAp-II were 0.015 and 0.082, respectively. SEM observation revealed that the precipitates were present as aggregates composed of primary particles of less than 1μm in diameter.

XRD patterns of NbHAps annealed at 800°C are shown in Fig.1(b). The crystalline of the precipitates become high by the annealing and XRD patterns of all annealed NbHAps could be identified as monolithic apatitic structure. It is noted that the crystallite of the NbHAp decreased as Nb content increased. Figure 2(a) shows an EDX spectra of the whole region of SEM image in Fig.2(b). The EDX spectrum from Nb M_α was separated from P K_α line and could be observed at 2.17KeV, although the intensity of the spectra was weak. The mapping image of Nb, Ca and P ions are shown in Fig.2(b). As shown in Fig.2(b), Nb ions were present at the same site of Ca and P ions. Based on these observations, Nb ions are suggested to be uniformly distributed in the

aggregates. High-resolution XPS spectrum of Nb $3d_{5/2}$ of NbHAp-II annealed at 800°C is shown in Fig.3. The peak of XPS spectra due to $3d_{5/2}$ of Nb ions from annealed NbHAp-II is at 208.3eV. Since XPS peak of $3d_{5/2}$ due to Nb^{2+} from NbO and Nb^{5+} from Nb_2O_5 appears at 203.5eV and 207.2eV, respectively, the Nb ions in NbHAp can be identified as Nb^{5+}.

These results suggest that the NbHAp has apatitic structure containing Nb ions and the Nb ions are homogenously distributed in the grain. Generally, Nb^{5+} ions in the solution is not present as Nb^{5+} but as niobiumate acid, $H_xNb_6O_{19}^{(8-x)-}$ ions (X=0,1,2)[4]. The PO_4 in HAp can be replaced by anionic atomic group, e.g. CO_3^{2-}, VO_4^{3-} and AsO_4^{3-}. Therefore, it is probable that Nb ions are substituted in PO_4 site in HAp. However, measured Nb/(Nb+P) molar ratio in NbHAp-II was 0.082, despite their theoretical Nb/(Nb+P) ratio of 0.1667, suggesting that the value of the measured ratio might be the maximum amount of Nb ions in PO_4, practically.

Since Nb ions are expected to have an effect to promote the proliferation and ALP activity of osteoblastic cells, the NbHAps have a potential to promote the ALP activity of osteoblastic cells.

Figure 4 shows ALP activity of NHOst cultured with annealed NbHAps. As shown in Fig.4, NHOst cultured with the NbHAp expressed the ALP activities twice as much as that of NHOst cultured with HAp without Nb ions. It is well known that ALP is often expressed when fracture of bone is repaired *in vivo*. Furthermore, from the recent study, it has revealed that the ALP contributed to mineralization in bone formation[5]. Therefore, this enhancement in ALP activity of NHOst by NbHAp suggests that the NbHAp can promote the mineralization of bone formation.

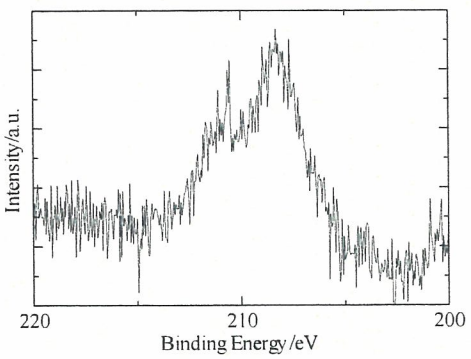

Fig.3. High-resolution XPS spectrum of Nb $3d_{5/2}$ of NbHAp-II annealed at 800°C.

Conclusion

We have succeeded to synthesize novel HAp containing Nb ions. The NbHAp would be a solid solution, which Nb ions were in PO_4 site in HAp and could enhance the ALP activity in NHOst.

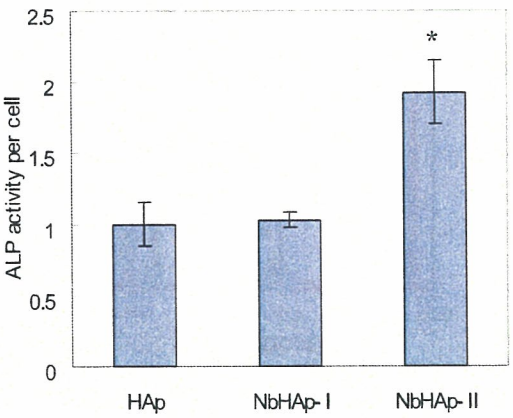

Fig.4. ALP activity of NHOst cultured with annealed NbHAp
*p<0.05 against HAp (without Nb ions)

Acknowledgment

This study was supported in part by a Grant-in-Aid for Scientific Research on Advanced Medical Technology from Ministry of Labour, Health and Welfare, Japan and a Grant-in-Aid from Japan Human Sciences Foundations.

References

[1] J.C.Elliott: *Structure and chemistry of the apatite and other calcium orthophosphates* (Elsevier, Tokyo, 1994)
[2] K.Isama, and T.Tsuchiya: Bull.Natl.Inst.Health.Sci., Vol.121 (2003) p.111
[3] T.Ohya, T.Ban, YOhya and Y.Takahashi: Ceram.Trans., Vol.112 (2001) p.47
[4] F.A.Cotton and G.Wilkinson: *Advanced Inorganic Chemistry* (Baifukan, Tokyo, 1994)
[5] H.Sowa, H.Kaji, T.Yamaguchi, T.Sugimoto and K.Ichihara: J.Bone.Miner.Res. Vol.17 (2002) p.1190

Key Engineering Materials Vols. 309-311 (2006) pp. 1293-1296
online at http://www.scientific.net

Enhancement of Differentiation and Homeostasis of Human Osteoblasts by Interaction with Hydroxyapatite in Microsphere Form

Ryusuke Nakaoka [a] and Toshie Tsuchiya [b]

Division of Medical Devices, National Institute of Health Sciences
1-18-1 Kamiyoga, Setagaya-ku, Tokyo 158-8501, JAPAN
[a] nakaoka@nihs.go.jp, [b] tsuchiya@nihs.go.jp

Keywords: osteoblasts, differentiation, homeostasis, hydroxyapatite, biocompatibility

Abstract. The aseptic loosening of artificial joints with associated periprosthetic bone resorption may be partly due to the suppression of osteoblast function to form new bone by wear debris derived from the joint. To assess the effect of wear debris on osteoblasts, we cultured normal human osteoblasts (NHOst) in contact with several kinds of microspheres as models of wear debris. The NHOst in contact with polystyrene, polyethylene, and alumina microspheres showed a lower differentiation level than NHOst alone as estimated from the amounts of deposited calcium. On the other hand, hydroxyapatite particles enhanced the differentiation of NHOst. In addition, sintered hydroxyapatite enhanced expression of osteocalcin mRNA and gap junctional communication of NHOst. This study suggests that polystyrene, polyethylene, and alumina microspheres have the potential to disorder not only the differentiation but also the homeostasis of NHOst in contact with them. However, hydroxyapatite enhanced the differentiation as well as the homeostasis of NHOst, even in microsphere form, suggesting its good biocompatibility as biomaterials for bone tissues.

Introduction

Biomaterials implanted into the harsh environment of the body cannot maintain their original shape, or even their desired function, resulting in undesirable side effects. One good example is the aseptic loosening of artificial joints observed in many patients who underwent a total joint replacement 5 to 25 years ago. Many researchers have reported that aseptic loosening with associated periprosthetic bone resorption is partly due to the activation of macrophages and osteoclasts by wear debris from the artificial joint [1-3], but few researches have focused on the interaction between wear debris and osteoblasts, especially normal human osteoblasts [4]. In this study, normal human osteoblasts were cultured in contact with various kinds of microspheres made from polymers or ceramics used as model wear debris, and the effects of the microspheres' characteristics and interaction conditions were discussed in regard to the proliferation, differentiation and homeostasis maintenance of the osteoblasts.

Materials and Methods

Microspheres. Monodispersed polystyrene (PS) microspheres with different diameters (0.1, 0.5, 1, 5, and 10 μm) were kindly supplied by Japan Synthetic Rubber Co., Ltd. (Tokyo, JAPAN). Low-density polyethylene (PE) microspheres were kindly provided by Sumitomo Seika chemicals Co., Ltd. (Tokyo, JAPAN). Alumina (Al_2O_3) microspheres were obtained from the Association of Powder Process Industry and Engineering. Sintered and un-sintered hydroxyapatite (HAp) microspheres (7.2 μm in diameter) were prepared and supplied by Ube Material Industries, Ltd. (Chiba, Japan). Determined by Multisizer II (Coulter Electronics Inc., Hialeah, FL), the average diameters of PE and alumina microspheres were found to be 6.4 and 5.1 μm, respectively. Sterile microspheres and microsphere-coated plates were prepared by the method previously reported [5]. The obtained microspheres and microsphere-coated plates (20 μg/well) were subjected to the assays.

Cellular Assays. Normal human osteoblasts (NHOst) were purchased from BioWhitteker Inc. (Walkersville, MD). The cells were maintained using alpha minimum essential medium (Gibco) containing 20% fetal calf serum (FCS) in incubators (37°C, 5%-CO_2-95%-air, saturated humidity).

All assays were carried out using the medium supplemented with 10mM β-glycerophosphate. NHOst ($2x10^4$ cells/well/500 µl medium) were cultured on the microsphere-coated plates for estimating the effect of the microspheres from the bottom of the cells. To estimate the effect of microspheres on cells adhered to the culture plates, the NHOst were cultured with microsphere-containing medium (20 µg/500 µl medium) after they had adhered to the collagen-coated plates. The cell number ratio of NHOst cultured with microspheres was evaluated using the alamar Blue™ assay (BioSource International, Inc., Camarillo, CA), which incorporates an oxidation-reduction indicator based on the detection of metabolic activity, according to manufacturer's instruction.

The level of alkaline phosphatase (ALP) activity of the NHOst and the amounts of calcium deposited during a 7-day incubation were evaluated to estimate differentiation level of NHOst as previously reported [6]. In addition, RT-PCR was performed to detect the expression of osteocalcin mRNA in the NHOst (primers for human osteocalcin [7]; forward 5'CATGAGAGCCCTCACA3' and reverse 5'AGAGCGACACCCTAGAC3'; product size 307-bp).

Gap junctional intercellular communication (GJIC), which is a function that plays an important role in maintaining cell and tissue homeostasis by exchanging low molecular weight molecules [8], among NHOst co-cultured with microspheres were evaluated using FRAP assay as previously reported [9].

All data were expressed as the mean value ± the standard deviation (SD) or the standard error of means (SEM) of the obtained data as indicated in all figures and tables. The Fisher-Tukey criterion was used to control for multiple comparisons and to compute the least significant difference between means.

Results and Discussion

Figure 1 shows the effect of the diameter of pre-coated polystyrene microspheres on proliferation, the ALP activity of co-cultured NHOst cells, and the amounts of deposited calcium on the NHOst. To compare the effect of the microspheres on the ALP activities and the calcium amounts for each NHOst, the obtained data were standardized based on the cell number ratio co-cultured with the microspheres. As shown in figure, suppression on ALP activity of NHOst and the amounts of deposited calcium were observed when 0.1 µm and 5 µm microspheres were co-cultured. When the microspheres were added after cell adhesion, they did not show a significant inhibitory effect on the functions of NHOst (data not shown). By pre-coating of the microspheres on the bottom of the test plates, the area they occupied became larger as their diameter became smaller. This increase in the microsphere occupied area would affect many functions of the test cells, resulting in the inhibitory effect of the 0.1µm microspheres on the function of NHOst when the same quantity of microspheres was coated. On the other hand, the suppression of ALP activity of NHOst and calcium deposition by pre-coated 5 µm PS microspheres suggests that not only the area they occupied but also their size may cause the unique inhibitory activity of the 5 µm PS microspheres. It is well known that the size of a microsphere plays an important role in phagocytosis [10], although it is unclear that there is the same size dependence on phagocytosis by the NHOst as by macrophages. In addition, our previous study suggested that even fibroblasts were likely to phagocyte microspheres of a specific

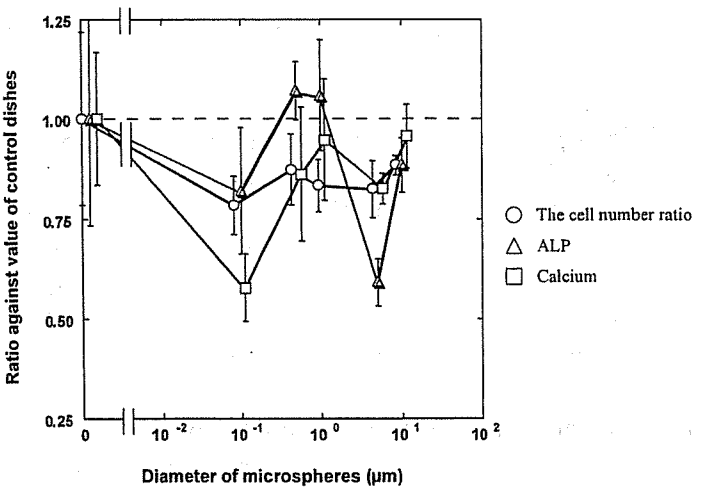

Figure 1. Effects of diameter of pre-coated PS on various functions of NHOst. Data are shown as the means±SD

diameter [5,9]. Taking into account our findings about the inhibitory effects of various microspheres on the functions of NHOst, it is probable that NHOst can phagocyte PS microspheres as well as macrophages, and in particular, may phagocyte microspheres 5 μm in diameter. Moreover, the effect of the added PS microspheres suggests that NHOst better recognize the microspheres from their lower than upper side. This may explain the reduced functions of NHOst co-cultured with the pre-coated 5 μm PS microspheres.

To estimate the effect of the material composing the microspheres, NHOst were cultured for 1 week on pre-coated PS, PE, alumina and HAp microspheres, all of which have a diameter of around 5 μm. Table 1 shows their number ratio and ALP activities, and the calcium amounts. Pre-coated PS, PE and alumina microspheres showed the potential to suppress functions of NHOst although some of these data did not show statistical differences against NHOst without microspheres. However, when NHOst were cultured with pre-coated HAp, the amount of calcium deposited was almost twice that detected in the cells without microspheres. It was observed that HAp microspheres have no potential to deposit calcium after a 1-week incubation without NHOst (data not shown). Therefore, the increase in calcium deposition by pre-coated HAp may be due to the enhancement in the differentiation of NHOst in contact with HAp. As expected, added various microspheres affected NHOst in a similar manner but less than the pre-coated microspheres (data not shown). We have hypothesized that GJIC of cells in contact with various biomaterials can be used as an index for estimating the biocompatibility of many kinds of biomaterials [5,6,9,11]. In addition, osteoblasts have been reported to communicate with one another *via* GJIC function, and the function is believed to be critical to the coordinated cell behavior necessary in bone tissue development [8,12]. Therefore, effects of these microspheres on the communication of co-cultured NHOst were estimated to consider the relation between this function and the differentiation of NHOst. The FRAP assay revealed that HAp microspheres enhanced the GJIC level of NHOst to 1.8 times as much as that of NHOst alone but others slightly inhibited it, indicating HAp has a potential to enhance homeostasis maintenance function of the NHOst as well as their differentiation. Details of the microspheres effects on GJIC of NHOst will be reported elsewhere [13]. These results indicated that the materials of microspheres affected the differentiation of co-cultured NHOst as well as the diameter of microspheres and their contact with the cells. In addition, microspheres made from HAp, which is a major component of bone tissue and has been shown to have good biocompatibility as bone substitute implants [14], may have the potential to enhance the differentiation of osteoblasts. These results suggest that the estimation of the effects of biomaterials in microsphere form on in vitro cell function may be useful for their in vivo biocompatibility evaluation.

We estimated the effect of sintering, normally used to harden HAp, on the function of NHOst. The estimation revealed that both HAp microspheres enhanced the amount of calcium deposited although the ALP activity of the cells decreased. In addition, when the un-sintered HAp microspheres were incubated with NHOst, the calcium deposition was observed more than sintered HAp. As another index of the differentiation of the NHOst, mRNA expression levels of osteocalcin, which is a well-known protein detected in

Table 1. Effects of a 1-week incubation with pre-coated microspheres on various functions of NHOst.
(Amounts of microspheres = 20 μg/well)

	Control	Polystyrene	Polyethylene	Alumina	Hydroxy Apatite (Sintered)
Diameter (μm)		5.0	6.4	5.1	7.2
The cell number ratio (%)	100.0±5.5	88.2±2.2	92.2±1.3	82.4±2.8	83.0±2.3
Percent ALP activity (activity/proliferation)	100.0±4.7	79.2±5.6	72.7±3.6*	58.2±5.7*	73.8±6.0*
Percent deposited calcium (Calcium percent/proliferation)	100.0±3.7	97.3±4.2	82.3±3.7	90.3±7.8	163.3±18.5*(a

Data are shown as the mean value ± SEM (n = 4 to 22)
* $p < 0.01$, against control group
(a) $p < 0.05$, against NHOst co-cultured with polyethylene and alumina microspheres

differentiated osteoblasts [15], were determined using the RT-PCR technique. Figure 2 shows time profiles of osteocalcin mRNA expression in NHOst cultured with pre-coated PS, PE, alumina, and two kinds of HAp microspheres. As shown in the figure, only the cells co-cultured with sintered HAp microspheres expressed osteocalcin mRNA after a 1-day incubation, while those co-cultured with other microspheres did not express the mRNA. This finding suggests that sintered HAp microspheres have the potential to induce osteocalcin production from NHOst. Neither spontaneous calcium deposition was observed by the incubation of sintered nor un-sintered HAp microspheres without NHOst, so that it is possible that the un-sintered HAp degrade in culture medium with NHOst, resulting in an increase of calcium concentration in the culture medium that enhances the calcium deposition by the NHOst. Therefore, it is suggested that sintered HAp can induce the differentiation of NHOst, and may be a suitable material for inducing osteogenesis rather than un-sintered one.

In conclusion, microspheres made from various materials had an effect on the differentiation of NHOst. The level of the effect varied with the size, amount, and composition of the microspheres. Microspheres made from PS, PE and alumina showed a potential to suppress the proliferation and the differentiation of co-cultured NHOst. On the other hand, microspheres made from HAp, especially sintered HAp, enhanced the differentiation of co-cultured NHOst, and showed their potential to maintain their homeostasis. Estimating the effect of various microspheres on the differentiation of osteoblasts will provide valuable information on the effects of wear debris from artificial hip joints as well as estimating their effects on osteoclast function.

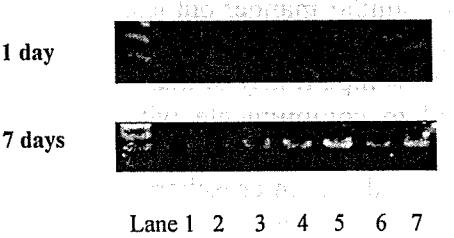

Figure 2. Expression of osteocalcin mRNA extracted from NHOst cultured on various microsphere pre-coated dish. Lane 1: Collagen-coated culture dish, 2: methanol-treated dish, 3: PS, 4: PE, 5: alumina, 6: un-sintered HAp, 7: sintered HAp.

Acknowledgements

We are grateful for the support of Health and Labor Sciences Research Grants for Research on Advanced Medical Technology, Research on Health Sciences focusing on Drug Innovation and Risk Analysis Research on Food and Pharmaceuticals, Ministry of Health, Labour and Welfare.

References

[1] J.A.Savio III, L.M.Overcamp and J.Black, Clin. Mater., **15,** 101 (1994)
[2] T.R.Green, J.Fisher, J.B.Matthews, M.H.Stone and E.Ingham, J. Biomed. Mater. Res. (Appl. Biomater.), **53,** 490 (2000)
[3] M.C.D.Trindade, D.J.Schurman, W.J.Maloney, S.B.Goodman and R.L.Smith, J. Biomed. Mater. Res., **51,** 360 (2000)
[4] C.Vermes et al., J. Bone. Miner. Res., **15,** 1756 (2000)
[5] R.Nakaoka, T.Tsuchiya, K.Sakaguchi and A.Nakamura, J. Biomed. Mater. Res., **57,** 279 (2001)
[6] M.Nagahata, R.Nakaoka, A.Teramoto, K.Abe and T.Tsuchiya, Biomaterials, **26,** 5138 (2005)
[7] M.M.Levy et al., Bone, **29,** 317 (2001)
[8] A.D.Maio, V.L.Vega and J.E.Contreras, J. Cell. Physiol., **191,** 269 (2002)
[9] R.Nakaoka and T.Tsuchiya, Mater. Trans., **43,** 3122 (2002)
[10] Y.Tabata and Y.Ikada, Adv. Polym. Sci., **94,** 107 (1990)
[11] T.Tsuchiya, J. Biomater. Sci. Polymer Edn., **11,** 947 (2000)
[12] H.J.Donahue, Z.Li, Z.Zhou and C.E.Yellowley, Am. J. Physiol. Cell Physiol., 278, C315 (2000)
[13] R.Nakaoka, S.Ahmed and T.Tsuchiya, J. Biomed. Mater. Res., in press
[14] K.Degroot, Biomaterials, **1,** 47 (1980)
[15] J.Chen, H.S.Shapiro and J.Sodek, J. Bone Miner. Res., **7,** 987 (1992)

Available online at www.sciencedirect.com
SCIENCE DIRECT®
Biomaterials 27 (2006) 1437–1443
Biomaterials
www.elsevier.com/locate/biomaterials

The effect of hyaluronic acid on insulin secretion in HIT-T15 cells through the enhancement of gap-junctional intercellular communications

Yuping Li[a,1], Tsutomu Nagira[a,b], Toshie Tsuchiya[a,*]

[a]*Division of Medical Devices, National Institute of Health Sciences, 1-18-1 Kamiyoga, Setagaya-ku, Tokyo 158-8501, Japan*
[b]*Japan Association for the Advancement of Medical Equipment, 3-42-6 Hongo, Bunkyo-ku, Tokyo 113-0033, Japan*

Received 28 April 2005; accepted 11 August 2005
Available online 19 September 2005

Abstract

The transplantation of bioartificial pancreas has the potential to restore endogenous insulin secretion in type I diabetes. The bioartificial pancreas is constructed in vitro from cells and a support matrix. Hyaluronic acid (HA) is an extremely ubiquitous polysaccharide of extracellular matrix in the body and plays various biological roles. It has been suggested that high molecular weight (HMW) HA increases in the function of gap-junctional intercellular communications (GJIC) and the expression of connexin-43 (Cx43). To determine whether the function of pancreatic β-cells is affected by gap junctions after HMW HA-treatment, we exposed HIT-T15, a clonal pancreatic β-cell line, in various concentrations of HA for 24 h, and then detected the insulin secretion and content, using an insulin assay kit by ELISA technique. The cellular functions of GJIC were assayed by dye-transfer method using the dye solution of Lucifer yellow. HA-treatment resulted in the enhancement of GJIC function, the increase of insulin release and insulin content. The results obtained in this study suggest that HA-coating increases the insulin secretion of HIT-T15 cells by the enhancement of Cx43-mediated GJIC. The results give useful information on design biocompatibility of HA when is used as a biomaterial for bioartificial pancreas.

Keywords: Hyaluronic acid; Gap-junctional intercellular communications; HIT-T15 cells; Insulin; Bioartificial pancreas

1. Introduction

Type I diabetes is caused by the autoimmune destruction of the β-cells. All patients with type I diabetes require daily insulin shots for the control of glucose levels. However, the insulin therapy cannot inhibit the development of serious chronic complications. The pancreas transplantation has been expected to be the most promising approach toward treating diabetes. The bioartificial pancreas is constructed in vitro from insulin-secreting cells or islets and a support matrix by a tissue engineering method. The frequently used matrix materials are alginate and agar [1,2]. Although bioartificial pancreatic constructs contain insulin-secreting cells entrapped in agar or alginate matrix implanted into the peritoneal cavity of the diabetic patient, mice, and dog, can restore normoglycemia and markedly abate diabetic symptoms, there are important questions in the structural integrity of support matrix, metabolic activity and viability of cells or islets, and late vascular thrombosis [1,2]. Therefore, the new matrix biomaterials, which mimic the functions of extracellular matrix (ECM), need to be researched.

Hyaluronic acid (HA) is an extremely ubiquitous member of the nonsulfated glycosaminoglycan ECM molecule family and is thought to play various biological roles particularly in growth, adhesion, proliferation, differentiation, and cell migration [3,4]. More importantly, the receptor for HA-mediated motility regulates gap-junction

*Corresponding author. Division of Medical Devices, National Institute of Health Sciences, 1-18-1 Kamiyoga, Setagaya-ku, Tokyo 158-8501, Japan. Tel.: +81 3 3700 9196; fax: +81 3 3700 9196.
E-mail address: tsuchiya@nihs.go.jp (T. Tsuchiya).
[1]Present address: School of Life Sciences, Nanchang University of Sciences and Technology, Nanchang, China.

0142-9612/$ - see front matter © 2005 Elsevier Ltd. All rights reserved.
doi:10.1016/j.biomaterials.2005.08.020

channel and connexin-43 (Cx43) expression by its actions on focal adhesions and the associated cytoskeleton [5]. In addition, Park and Tsuchiya [6] have reported that high molecular weight (HMW) HA-coating can enhance the function of gap-junctional intercellular communications (GJIC). The insulin secretion from pancreatic β-cells is a multicellular event depending on their interaction with neurotransmitters and numerous signal molecules carried by blood and also direct interactions between cell–cell and cell–matrix contacts by gap-junctional channels, which mediate exchanges of molecules smaller than 1000 Da, such as ions, small metabolites, and second messengers between adjacent cells. The latter interactions are thought to be crucial regulatory mechanisms of insulin secretion [7–9], and the pharmacological blockade of GJIC markedly decreases insulin release [8]. However, the effects of HMW HA as biomaterials of support matrix on functions of pancreatic β-cells and gap-junctional channel remain unclear.

In the present study, we investigated the effects of HMW HA on the function of GJIC, the expression of Cx43, insulin content, and insulin secretion using HIT-T15 cells in vitro. These results suggest that HMW HA can be used as the biomaterial for the development of a bioartificial pancreas: design biocompatibility of HA depends on the molecular-weight size of HA, and its application method and concentration.

2. Materials and methods

2.1. Materials

Lucifer yellow was purchased from Molecular Probes (Eugene, OR). HA (1680 kDa) and TetraColor ONE (WST-8) were supplied by Seikagaku Industries, Ltd. (Tokyo, Japan). ELISA insulin assay kit was obtained from Morinaga Seikagaku Co. (Yokohama, Japan). Bovine serum albumin (BSA) was obtained from Roche Diagnostics GmbH (Mannheim, Germany). Krebs–Ringer bicarbonate (KRB) buffer (pH 7.4), fetal bovine serum (FBS), and anti-Cx43 were purchased from Sigma Chemical Co. (St. Louis, MO). β-actin antibody was obtained from Cell Signaling Technology Inc. (Tokyo, Japan). Roswell Park Memorial Institute (RPMI) 1640 medium was from Nissui pharmaceutical Co. (Tokyo, Japan). All other chemicals used were obtained from Wako Pure Chemical Industries (Osaka, Japan).

2.2. Preparation of media and culture dishes

The HA polysaccharide was dissolved in distilled water at a concentration of 4 mg/ml. Each of the 35-mm culture dish (Falcon 1008, Becton Dickinson) was coated at a final concentration of 0.01, 0.05, 0.1, 0.5, and 1.0 mg/ml. The HA-coated dishes were dried further under sterile air flow at room temperature for 12 h before use. In order to investigate the effect of HA-addition on the functions of HIT-T15 cells, different media were prepared at a final concentration of 0.01, 0.05, 0.1, 0.5, and 1.0 mg/ml. HA-treatment is performed to cells for 24 h.

2.3. Cells and cell culture

A hamster pancreatic β-cell line, HIT-T15 (HIT-T15 cells, Dainippon Pharmaceutical Co., Japan), was cultured in RPMI 1640 medium containing 10% FBS, 2 mM L-glutamine, 100 IU penicillin-G and 100 μg/ml streptomycin at 37 °C in a humidified atmosphere of 5% CO_2. The subculture cells were seeded at a density of $1.0–5.0 \times 10^5$ cells/ml in multiwell plates or culture dishes. When they reached more than 80% confluence, the cells were used for various studies. Throughout the cell growth period the culture media were replaced every 2 days.

2.4. Measurement of cell viability

To evaluate the affect of HMW HA on cell viability of HIT-T15 cells, HIT-T15 cells (1×10^5) were incubated into the various concentrations of HA-coated 24-well plates, or after the cells were seeded onto 24-well plates and pre-incubated in a 10% FBS/RPMI 1640 medium overnight, the medium was exchanged for 10% FBS/HA/RPMI 1640 medium prepared. After 24 h of HA-treatment, the cell viability was determined by the WST-8 reduction assay, according to the manufacturer's instructions. Control cells received fresh medium without HA.

2.5. Measurement of insulin release and insulin content

HIT-T15 cells were treated as described above. After pre-incubating for 30 min at 37 °C in KRB buffer, no glucose cells were stimulated for 60 min with 11.1 mM glucose in KRB buffer. The medium was collected, centrifuged for 5 min at 3000*g*, and the supernatant was frozen at −80 °C for insulin release assay. Cultures were then extracted for 24 h at 4 °C in acid-ethanol and the extracts also frozen for determination of insulin and protein content. Insulin was determined by ELISA insulin kit with rat insulin as standard, according to the manufacturer's instructions. Protein content was measured by the BCA protein assay reagent kit with albumin as standard (PIERCE). Values of secreted insulin were normalized to protein content.

2.6. Measurement of dye transfer

Gap junction-mediated communication between β-cells regulates the insulin secretion and insulin biosynthesis. Because HMW HA-coating increased the insulin release and insulin content but not HA-added, we tested whether the HA-coating increases the insulin secretion and insulin content have a relationship with gap junctions between HIT-T15 cells. HIT-T15 (5×10^5) cells were exposed to the HA-coated (0.1, 0.25, and 0.5 mg/dish) 35-mm glass coverslip (Ashland, MA) and incubated for 24 h to evaluate dye coupling using Lucifer yellow. The cells were rinsed with phosphate-buffered saline [PBS(+)] containing Ca^{2+}/Mg^{2+}, and 3 ml of PBS(+) containing 1% BSA and 10 mM HEPES (pH 7.4) were added to keep a sufficient pH stability under the microscope. The junctional coupling of HIT-T15 cells was determined by injecting Lucifer yellow into individual cells within monolayer clusters. Injections were performed on a phase-contrast microscope with InjectMan NI2 and microinjector FemtoJet (Eppendorf AG, Germany) using glass micropipette that were filled with a 4% solution of Lucifer yellow CH (MW 457.2) dissolved in 0.33 M lithium chloride, as previously described [11]. An injection pressure of 6.5 psi for 200 ms was used for each injection. The coupling extent was evaluated by counting dye-transferred cells at 2 min after microinjection. There was no leakage of injected dye into the medium.

2.7. Western blot analysis

HIT-T15 cells were grown into the various concentration of HA-coated 100-mm plastic dishes (0.1, 0.25, and 0.5 mg/dish) (FALCON 3003; Falcon) for 24 h, rinsed with Ca^{2+}/Mg^{2+}-free PBS(−) and then lysed in CelLytic™-M lysis/extraction reagent (Sigma). Protein content was measured by the BCA protein assay reagent kit (PIERCE). Samples of total extracts (20 μg protein/lane) were fractionated by eletrophoresis in a 10% sodium dodecyl sulfate polyacrylamide gel electrophoresis (SDS–PAGE). The contents of the gels were transferred to PVDF membranes (Clear Blot Membrane-P). Membranes were saturated for 2 h at room temperature in Block Ace (Dainippon Pharmaceutical Co.,

Japan) and then were incubated with antibodies directed against Cx43 (1:1000) and β-actin (1:1000) as the primary antibody overnight at 4 °C. After repeated rinsing in PBS–Tween, the immunoblots were incubated with a peroxidase-conjugated antibody against rabbit (1:5000) at room temperature for 1 h. Membranes were developed by enhanced chemiluminescence according to the manufacturer's instructions (Amersham Pharmacia Biotech).

3. Results

3.1. Cell viability

In order to evaluate the affect of HMW HA on cell viability, HIT-T15 cells were incubated with HA-coated (0.01, 0.05, 0.1, 0.5, and 1.0 mg/dish) or -added (0.01, 0.05, 0.1, 0.5, and 1.0 mg/ml) for 24 h. After 24 h exposure to HA-added, there was no significant change in the viable HIT-T15 cell number at the low concentration of HA-added ($\leqslant$1.0 mg/dish) compared to control. In contrast, after 24 h of incubation, the cell viability of HIT-T15 cells grown on high concentration HA-coated dishes ($\geqslant$1.0 mg/dish) was significantly less than on low concentration HA-coated and control (Fig. 1). Therefore, all further studies were conducted using low concentration of HA ($\leqslant$0.5 mg/dish).

3.2. Insulin secretion and insulin content

HIT-T15 cells, retain glucose-stimulated insulin secretion, showed an increase in insulin secretion as a function of stimulation. Thus, their insulin output was 2.73±0.36 and 3.90±0.41 pg/μg protein in the base and glucose-stimulation (11.1 mM), respectively ($n = 9$ dishes from three independent experiments). When these cells were exposed to a low concentration of HA-coating (0.1, 0.25, and 0.5 mg/dish) for 24 h, their insulin secretion was significantly increased in the presence of glucose-stimulation (Fig. 2). However, in contrast, when HIT-T15 cells were incubated with HA-addition for 24 h, the increasing effect was not exhibited. The insulin secretion was without a difference between control and HA-addition (Fig. 2). On the other hand, after acid-ethanol extraction, we found that the insulin content of the HIT-T15 cells grown onto the HA-coated dishes was significantly increased but not HA-added (Fig. 3).

GJIC and Cx43 are thought to be crucial regulatory mechanisms of insulin secretion and insulin content. As described above, HA-coating increased insulin secretion and insulin content of the HIT-T15 cells. In addition, Park and Tsuchiya [6] reported that HMW HA-coating can enhance the function of GJIC in normal human dermal fibroblasts but not HA-addition. Hence, all further studies on the mechanism of insulin secretion and insulin content were conducted using HA-coating.

3.3. Dye transfer

We assessed the function of GJIC using Lucifer yellow by counting the number of dye-transferred cells at 2 min

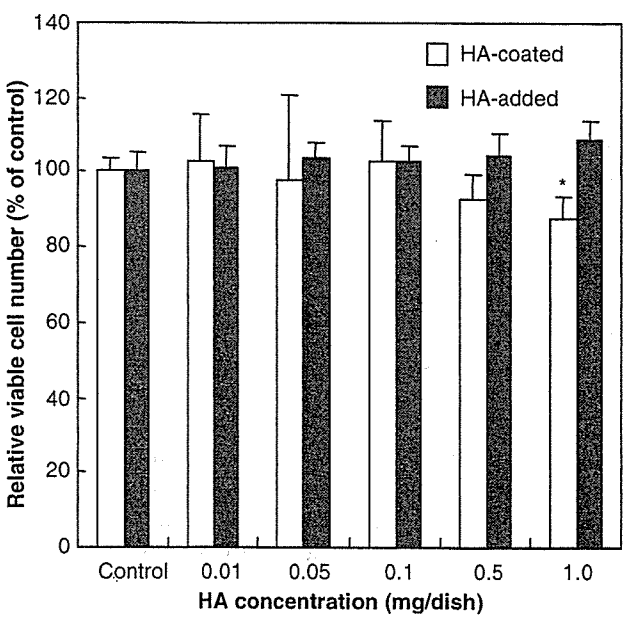

Fig. 1. Concentration-dependent effects of HA-treatment on viability of HIT-T15 cell. After HIT-T15 cells were incubated with HA-coated or HA-added for 24 h, the viable cell numbers of HIT-T15 cell were determined by WST-8 assay as described in methods. Each value denotes the mean±S.D. of three separate experiments. *$P \leqslant 0.05$ compared to control under the HA-coated condition.

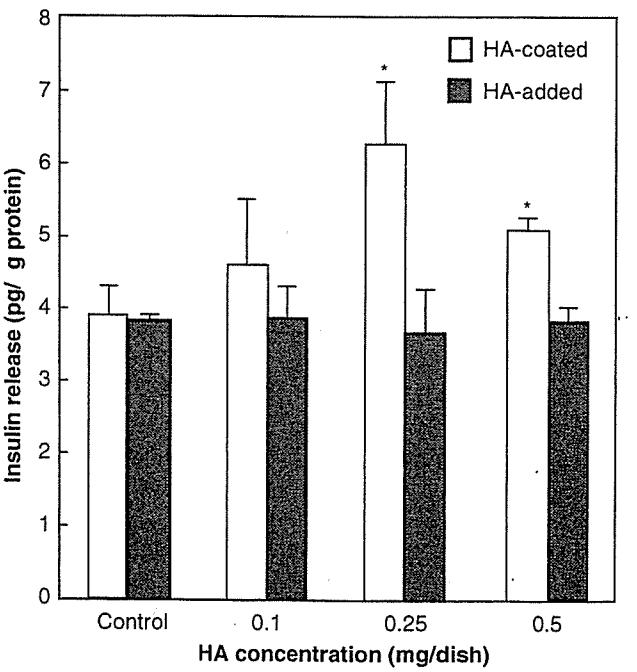

Fig. 2. Insulin secretion from HIT-T15 cells by HA-treatment. HIT-T15 cells were incubated with HA-coating (□) or HA-added (■) for 24 h and then stimulated for 60 min with 11.1 mM glucose in KRB buffer. The released insulin in the spent medium was determined by ELISA insulin kit. Each value denotes the mean±S.D. of three separate experiments. *$P \leqslant 0.05$, compared to control in the presence of glucose.

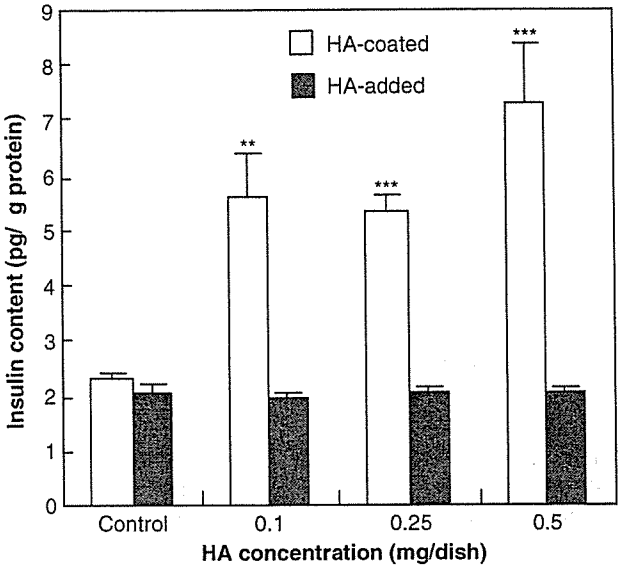

Fig. 3. Insulin content of HIT-T15 cells incubated with HA-coated (□) and HA-added (■). Cells were incubated in the presence of different HA concentrations (0.1–0.5 mg/dish) for 24 h and then stimulated for 60 min with 11.1 mM glucose. The insulin content in the extracts was determined by ELISA insulin kit. Each value denotes the mean ± S.D. of three separate experiments. $^{**}P \leqslant 0.01$ and $^{***}P \leqslant 0.001$ compared to control.

after microinjection. Fig. 4A shows the patterns of dye transfer in HIT-T15 cells treated with HA-coating (0.1, 0.25, and 0.5 mg/dish) for 24 h. Most microinjections led to the intercellular transfer of Lucifer yellow, indicating the frequent coupling of HIT-T15 cells. Under control conditions, microinjection experiments revealed that 47.1% of HIT-T15 cells transferred Lucifer yellow with a limited number (1.5 ± 0.6) of microinjection cells. In HA-coated conditions, almost injected cells (95%) showed Lucifer yellow dye transfer, the number of Lucifer yellow-transferred cells (3.2 ± 1.3, 4.4 ± 1.9, and 4.1 ± 1.9, respectively) was more than that of the control condition ($P < 0.001$) (Fig. 4B), which indicated that GJIC function was activated by the HA-coating.

3.4. Cx43 expression

Cx43 is the 43-kDa member of a conserved family of membrane spanning gap-junction proteins. To provide further evidence that the HA-coating increased the function of GJIC, relative to the levels of actin, comparable levels of immunolabeled Cx43 was detected in 0.1, 0.25, and 0.5 mg/dish of HA-coating cells. Whole cell lysates from HA-coated dish were subjected to SDS–PAGE. Immunoblot analysis was performed with an antibody that specifically recognized Cx43 or β-actin. A Western blot analysis revealed that Cx43 proteins are present in cultured HIT-T15 cells in three forms at 43 kDa region, consisting of a nonphosphorylated form and phosphorylated forms (P1 and P2). HA-coating appeared to induce a greater concentration-dependent increase in all three Cx43 protein levels than control. However, the protein level of β-actin was no different from them (Fig. 5), indicating HA-coating increases the function of GJIC via the expression of Cx43. To account for differences in loading, proteins were both stained with Coomassie blue and immunolabeled for β-actin. The latter staining, which did not change in our experiments relative to that of Coomassie blue (data not shown), was used as an internal standard. These results suggested that HA-coating specifically increased the Cx43 protein but not all cell proteins of HIT-T15 cells.

4. Discussion

The transplantation strategy of bioartificial pancreas is to construct bioartificial tissues in vitro from cells or islets and a support matrix and implant the construct into the body in place of the original. The support matrix must be able to maintain the functions of differentiated cells or contain and/or be able to release appropriate biological signaling information to promote and maintain cell adhesion and differentiation. HA is a high-molecular-mass polysaccharide of support matrix in the body, which is believed to play roles in maintaining various physiological functions including water and plasma protein homeostasis, cell proliferation, cell locomotion, and migration [3]. HA is plentiful, easy to extract and mold into a variety of shape, and biodegradable. It is thus widely used matrix biomaterial for bioartificial tissues [10]. In this study, we investigated whether administration of various concentration of HMW HA influences the viability, GJIC, and insulin secretion of pancreatic β-cells as a matrix biomaterial of bioartificial pancreatic constructs.

Previous study has shown that HMW (310 and 800 kDa) HA-coating (2.0 mg/dish) resulted in low adhesiveness to the cells and the decrease of viability in normal human dermal fibroblasts, because of the change in GJIC functions and induction of various genes including cytokines, adhesion molecules, and growth factors [6,11,12]. In the present study, similar results were obtained. After 12 h, the HIT-T15 cells grown into low concentration HA-coated dishes (0.1, 0.25, and 0.5 mg/dish) and control cells already had attached and confluent but not high concentration HA-coated dishes ($\geqslant 1.0$ mg/dish). We showed that treatment with high concentration of HMW (1680 kDa) HA-coated dose dependently inhibited the viability of HIT-T15 cells. In contrast, there was no difference in viability of HIT-T15 cells between the control and HA-added dishes. These results indicated that among the individual qualities of ECM, the viscosity plays a decisive role. The changes of cell viability by HA-treatment may depend on the cell attachment activity. The difference in cell attachment activity may depend on the surface structure of the coated HA, because the HMW HA-coated surface provides a stable anionic surface that prevents cells attachment at the early time [13]. This result suggests that the molecular-weight size of HA and its

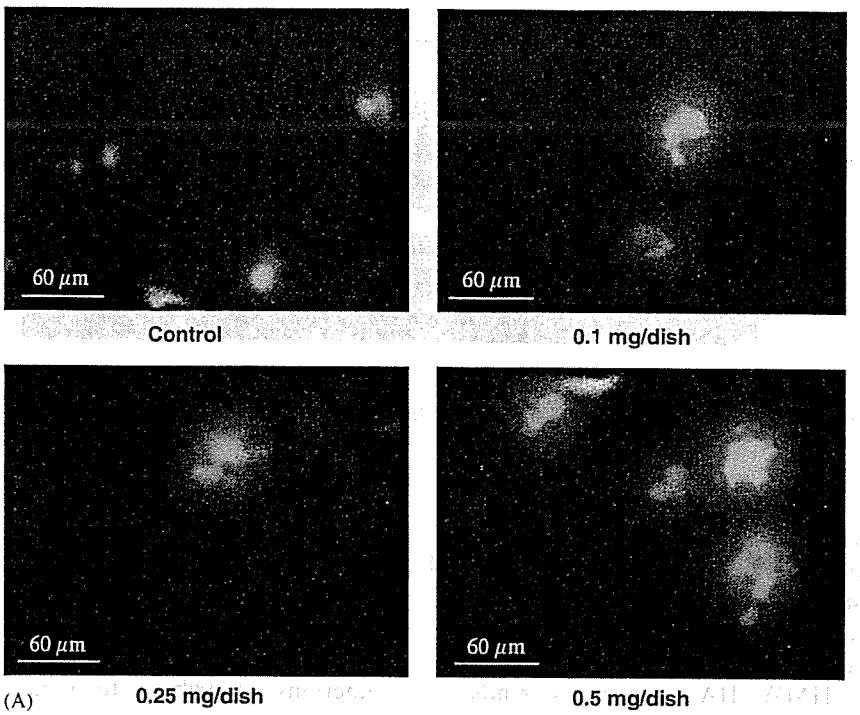

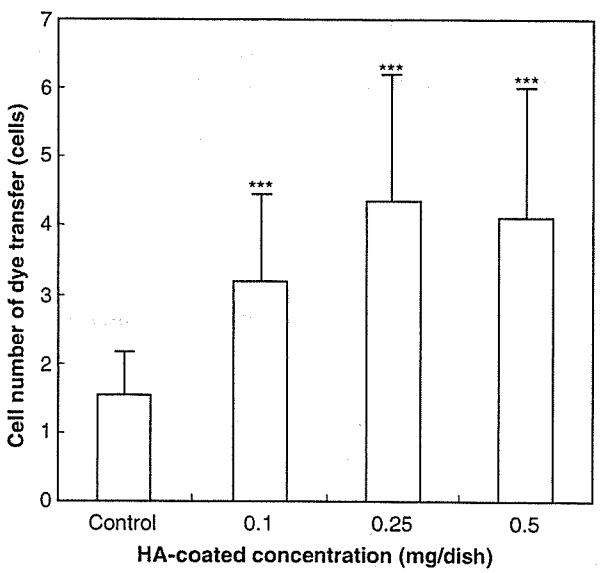

Fig. 4. Concentration-dependent effects of HA-coating on dye transfer in HIT-T15 cells. Cell adherent to glass coverslips were microinjected with 4% Lucifer yellow. Transfer of dye to neighboring cells was assessed by epifluorescence microscopy 2 min later. This is a representative expression of 18 injections per group (A). The number of neighboring cells that received dye was quantified (B). Each value expressed as the mean ± S.D. ($n = 18$). $^{***}P \leqslant 0.001$ compared to control.

application method and concentration are important factors for generating biocompatible tissue-engineered products.

It has been reported that single β-cells (which cannot form gap junctions) show alterations in both basal and stimulated release of insulin, in protein biosynthesis, and in the expression of the insulin gene. The sustained stimulation of insulin release is associated with an increase in β-cells coupling, in the expression of gap junctions by a unique mechanism for direct equilibration of ionic and molecular gradients between nearby cells [14–16]. In this study, we found that the insulin release and insulin content are increased and GJIC activity was enhanced in cultured HIT-T15 cells by low concentration HMW HA-coating in spite of the inhibitory effects on the cell viability in high concentration HA-coating dishes. This finding was consistent with previous reports. The effect of HA may be influenced by the viscosity of HA, the concentration of

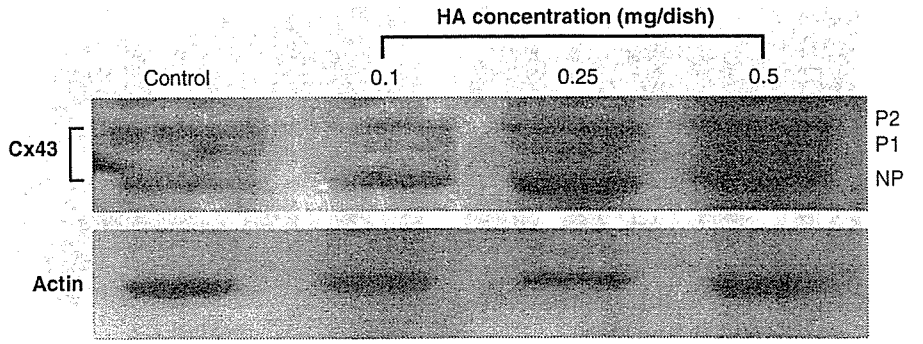

Fig. 5. Identification of Cx43 in HIT-T15 cells grown on the HA-coating dish by Western blot analysis. After HIT-T15 cells were incubated into HA-coated dish for 24 h, cells were lysed and proteins (20 μg) were separated by SDS–PAGE followed by Western blotting using rabbit anti-Cx43 antibody. Actin immunostaining was used to assess equivalent protein loading. This is a representative autoradiogram of three experiments.

FBS and the nutrients in media such as hormone, growth factor (FGF, etc.), cell adhesion molecule (N-CAM and cadherins), and transportation protein [6,17]. As a result, the HIT-T15 cells can use these nutrients and the nutrient-enriched substrata (e.g. natural ECMs) by ionic interaction and the binding of HMW HA to various kinds of cytokines, to change the cell aggregations, resulting in the increase of GJIC. With the evidence above, the enhancement of GJIC activity induced by HA-coating participated in the regulation of insulin release and insulin biosynthesis. On the other hand, the glucose stimulus-secretion coupling in β-cells generated several signals, including a signal to secrete preformed insulin stored in secretory vesicles, a signal, which may be the same or different, to secrete newly made insulin, and a signal to synthesize more insulin. The mechanism of glucose-induced insulin secretion is distinct from that of glucose-induced proinsulin biosynthesis and insulin gene transcription [18]. Moreover, the qualities of ECM affect the insulin release [19]. Therefore, it is possible that HA-coated dishes promoted a large increase in insulin synthesis but only a modest increase in insulin release. The detailed action mechanism should be investigated in the next study.

In native and tumoral insulin-producing pancreatic β-cells, gap-junction protein Cx43 has been identified. Furthermore, the stable transfection of the gene coding for Cx43 induces the expression of functional gap-junction channels and improves both the biosynthetic and secretory defects of the cells. Cx43-transfection and incidence of junctional coupling also secrete more insulin than wild-type and noncommunicating cells, the absence of Cx43 implicated in the loss of β-cell-specific functions in vitro and in vivo [9,14]. In this study, HA-coating expressing high levels of the Cx43, gap junctions, and coupling, showed the striking enhancement of the amounts of stored hormone in HIT-T15 cells and promoted the glucose-induced insulin release, indicating that adequate levels of Cx43 and coupling are required for proper insulin production. These results provide further evidence that HA-coating increases the pancreatic β-cells function by enhancing the function of Cx43-mediated GJIC.

5. Conclusion

In conclusion, the function of GJIC is considered to be a useful marker for evaluating tissue-engineered products. The data obtained in this study show that gap junctions contribute to regulating some still-unknown mechanism to couple the stimulus-secretion of HIT-T15 cells under the condition of low concentration HA-coating. The growth regulation with a bioartificial pancreatic construct using HA is achievable. These results give useful information on design biocompatibility of HA when the HA is used as a biomaterial for bioartificial pancreas. HA-coating may be a new technique for constructing three-dimensional bioartificial pancreas in tissue engineering.

Acknowledgements

This work was supported in part by a Grant-in-Aid for Scientific Research on Advanced Medical Technology from Ministry of Health, Labour and Welfare, Japan and a Grant-in-Aid from Japan Human Sciences Foundations.

References

[1] Soon-Shiong P, Heintz R, Yao Q, Yao Z, Zheng T, Murphy M, et al. Insulin independence in a type 1 diabetic patient after encapsulated islet transplantation. Lancet 1994;343:950–1.
[2] Maki T, Monaco AP, Mullon CJP, Solomon BA. Early treatment of diabetes with porcine islets in a bioartificial pancreas. Tissue Eng 1996;2:299–306.
[3] Laurent TC, Fraser JR. Hyaluronan. FASEB J 1992;6(7):2397–404.
[4] Knudson CB, Knudson W. Hyaluronan-binding proteins in development, tissue homeostasis, and disease. FASEB J 1993;7(13):1233–41.
[5] Nagy JI, Hossain MZ, Lynn BD, Curpen GE, Yang S, Turley EA. Increased connexin-43 and gap junctional communication correlates with altered phenotypic characteristics of cells overexpressing the receptor for hyaluronic acid-mediated motility. Cell Growth Differ 1996;7(6):745–51.
[6] Park JU, Tsuchiya T. Increase in gap-junctional intercellular communications (GJIC) of normal human dermal fibroblasts

(NHDF) on surfaces coated with high-molecular-weight hyaluronic acid (HMW HA). Inc J Biomed Mater Res 2002;60(4):541–7.
[7] Meda P. The role of gap junction membrane channels in secretion and hormonal action. J Bioenergy Biomembr 1996;28(4): 369–77.
[8] Meda P, Bosco D, Chanson M, Giordano E, Vallar L, Wollheim C, et al. Rapid and reversible secretion changes during uncoupling of rat insulin-producing cells. J Clin Invest 1990;86(3): 759–68.
[9] Vozzi C, Ullrich S, Charollais A, Philippe J, Qeci L, Medz P. Adequate connexin-mediated coupling is required for proper insulin production. J Cell Biol 1995;131(6 Part 1):1561–72.
[10] Hubbell JA. Materials as morphogenetic guides in tissue engineering. Curr Opin Biotechnol 2003;14(5):551–8.
[11] Park JU, Tsuchiya T. Increase in gap junctional intercellular communications by high molecular weight hyaluronic acid associated with fibroblast growth factor 2 and keratinocyte growth factor production in normal human dermal fibroblasts. Tissue Eng 2002;8(3):419–27.
[12] Nakamura K, Yokohama S, Yoneda M, Okamoto S, Tamaki Y, Ito T, et al. High, but not low, molecular weight hyaluronan prevents T-cell-mediated liver injury by reducing proinflammatory cytokines in mice. J Gastroenterol 2004;39(4):346–54.
[13] Forrester JV, Balazs EA. Inhibition of phagocytosis by high molecular weight hyaluronate. Immunology 1980;40(3):435–46.
[14] Meda P, Chanson M, Pepper M. In vivo modulation of connexin-43 gene expression and junctional coupling of pancreatic β-cells. Exp Cell Res 1991;192(2):469–80.
[15] Charollais A, Gjinovci A, Huarte J, Bauquis J, Nadal A, Martin F, et al. Junctional communication of pancreatic beta cells contributes to control of insulin secretion and glucose tolerance. J Clin Invest 2000;106:235–43.
[16] Meda P, Pepper MS, Traub O. Differential expression of gap junction connexins in endocrine and exocrine glands. Endocrinology 1993; 133(5):2371–8.
[17] Charollais A, Serre V, Mock C, Cogne F, Bosco D, Meda P. Loss of α_1 connexin does not alter the prenatal differentiation of pancreatic β-cells and leads to the identification of another islet cell connexin. Dev Genet 1999;24(1–2):13–26.
[18] Barton W, Cristina A, Isabelle B, Melissa KL, Christopher JR. Glucose-induced translational control of proinsulin biosynthesis is proportional to preproinsulin mRNA levels in islet β-cells but not regulated via a positive feedback of secreted insulin. J Biol Chem 2003;278(43):42080–90.
[19] Lim F, Sun AM. Microencapsulated islets as bioartificial endocrine pancreas. Science 1980;210:908–10.

Available online at www.sciencedirect.com
SCIENCE DIRECT®
ELSEVIER
International Journal of Pharmaceutics 303 (2005) 104–112
international journal of pharmaceutics
www.elsevier.com/locate/ijpharm

Reducing the migration of di-2-ethylhexyl phthalate from polyvinyl chloride medical devices

Rie Ito [a], Fumie Seshimo [a], Yuji Haishima [b], Chie Hasegawa [b], Kazuo Isama [b], Takeshi Yagami [b], Keisuke Nakahashi [c], Haruko Yamazaki [a], Koichi Inoue [a], Yoshihiro Yoshimura [d], Koichi Saito [a], Toshie Tsuchiya [b], Hiroyuki Nakazawa [a,*]

[a] *Department of Analytical Chemistry, Faculty of Pharmaceutical Sciences, Hoshi University, 2-4-41 Ebara, Shinagawa-ku, Tokyo 142-8501, Japan*
[b] *Division of Medical Devices, National Institute of Health Sciences, 1-18-1 Kamiyoga, Setagaya-ku, Tokyo 158-8501, Japan*
[c] *Terumo Corporation, 2-44-1 Hatagaya, Shibuya-ku, Tokyo 151-0072, Japan*
[d] *Department of Analytical Chemistry, Nihon Pharmaceutical University, 10281 Komuro, Ina, Kita-adachi-gun, Saitama 362-0806, Japan*

Received 12 April 2005; received in revised form 5 July 2005; accepted 10 July 2005
Available online 31 August 2005

Abstract

We attempted to determine the processing conditions for decreasing the migration of phthalate esters, particularly di-2-ethylhexyl phthalate (DEHP), from polyvinyl chloride (PVC) products using a drug solvent after dilution based on the package insert. PVC sheets and PVC tubing were subjected to optical irradiation (ultraviolet (UV), visible light irradiation) and heat treatment to determine whether they are deteriorated by these treatments. UV irradiation to one side of the PVC sheet decreased the levels of DEHP migration from the sheets by almost 50%, although the amount of DEHP content in PVC sheet was observed no significant change. On the other hand, the levels of DEHP migrating from the inner surface of PVC tubing UV-irradiated from the outer surface were not decreased compared with the control. Therefore, the surface structure was examined by conducting Fourier transform infrared spectroscopy (FT-IR), electron spectroscopy for chemical analysis (ESCA) and static angle of contact measurement. In FT-IR analysis, we found that the UV-irradiated PVC sheets were exhibited broadened absorption bands with time. In ESCA analysis, the chlorine content was decreased and the oxygen content was increased with time in UV-irradiated PVC sheets. Moreover, the other treated PVC sheets shows no significant change compared with the non-UV-irradiated PVC sheet. Therefore, the surface structure of the UV-irradiated PVC sheet was changed. As a result, the migration of DEHP from PVC products can be decreased with simple treatment, such as UV-irradiation. This could be a useful method to develop novel PVC products.

Keywords: Di-2-ethylhexyl phthalate (DEHP); Polyvinyl chloride (PVC); Medical device; UV irradiation; Surface structure

* Corresponding author. Tel.: +81 3 5498 5763; fax: +81 3 5498 5062.
E-mail address: nakazawa@hoshi.ac.jp (H. Nakazawa).

0378-5173/$ – see front matter © 2005 Elsevier B.V. All rights reserved.
doi:10.1016/j.ijpharm.2005.07.009

1. Introduction

Phthalate esters are widely used as industrial plasticizers. In particular, di-2-ethylhexyl phthalate (DEHP) is used in the manufacture of polyvinyl chloride (PVC) products and other plastics to achieve the desired softness, flexibility and stability for specific applications. PVC is employed in the production of floor tiles, food wrapping film, industrial tubing, and medical devices (Huber et al., 1996), and is the most widely used polymer because of its availability. In general, PVC products used in medicine contain up to 40% by weight of this plasticizer (Ljunggren, 1984); however, it has been reported that some species of phthalate esters including DEHP exhibit reproductive and developmental toxicity (Arcadi et al., 1998; Gray et al., 1999). DEHP is not chemically bound to the PVC polymer and may leach when a medical device is heated or when the PVC comes in contact with surrounding media, such as blood, serum, plasma, drugs and intravenously administered fluids. The migration of DEHP from PVC medical devices into the surrounding media has been reported to result in toxicity (Tickner et al., 2001; Yakubovich and Vienken, 2000; Hill et al., 2001). Extraction occurs either by leaching or after an extracting material (blood, IV fluid) diffuses into the PVC matrix and dissolves the plasticizer, which is relatively lipophilic (Rock et al., 1986). In Japan, the Ministry of Health, Labour and Welfare has set the tolerable daily intake (TDI) of DEHP at 40–140 μg/kg/day (MHLW, 2000) and the use of DEHP as a plasticizer has been regulated so that it cannot be used in the manufacture of, for example, infant toys and plastic gloves for handling food. DEHP has been reported to leach from PVC medical devices containing fat-soluble drugs to be administered orally. Depending on the conditions at the time of use, a patient may be exposed to high levels of DEHP through medical treatment (USFDA, 2001; Health Canada, 2002).

Many studies have been reported on the release behavior of DEHP from PVC medical devices under various conditions (Hanawa et al., 2000; Jenke, 2001; Faouzi et al., 1995), because it is essential that the exposure be precisely determined in order to evaluate its significance as an integral part of the risk assessment of DEHP to human health. However, the quality change of PVC products during storage has been not estimated so far. It is possible that the content and release behavior of DEHP may be influenced by optical irradiation and temperature change during storage. Moreover, in this study, a DEHP migration test using PVC products treated with optical irradiation (visible and ultraviolet) and heating as external factors during storage was performed using a drug solvent for injection after dilution to the required concentration based on the package insert. In addition, the surface structure was examined by conducting Fourier transform infrared spectroscopy (FT-IR), electron spectroscopy for chemical analysis (ESCA) and static angle of contact measurement. When the PVC products were irradiated with UV, degradation occurred (Takeishi and Okawara, 1970). The tensile test was also performed as PVC products may deteriorate due to irradiation and heat treatment. The results of this study led to the development of processing conditions for decreased DEHP migration from PVC products, and provided novel information relevant to risk assessment and product development.

2. Materials and methods

2.1. Materials and chemicals

The test materials were a medical PVC sheet (1 cm × 3 cm, thickness: 0.4 mm) used in the manufacture of blood bags, and PVC tubing (length 10 cm, i.d. 2.13 mm) used for the transfusion, infusion, and donation of blood.

The drug solvent used for the DEHP migration tests was Sandimmun® (250 mg cyclosporine per ampoule (5 ml), Novartis Pharma Co., Tokyo, Japan). It is used for injection after dilution with 50 mg/ml glucose to the required concentration (0.5 mg/ml as cyclosporine concentration) based on the package insert.

Phthalate esters, di-2-ethylhexyl phthalate and DEHP-d_4, were purchased from Kanto Chemical Co. (Tokyo, Japan). Hexane, anhydrous sodium sulfate, a sodium salt of DEHP analytical grade, analytical grade diethyl ether, and HPLC grade distilled water were used in the experiments.

2.2. Pretreatment of PVC sheet and tubing

2.2.1. Control

A PVC sheet maintained in the shade and at room temperature was used as a negative control.

2.2.2. Heat treatment

The PVC sheets were kept at temperatures of 4, 37 and 60 °C for 1 week, 2 weeks, 1 month, 2 months and 3 months. The positive control was a PVC sheet kept at 100 °C for 25 days.

2.2.3. Optical irradiation

The embossed side is the outer surface of a blood bag. Some PVC sheets were irradiated with visible light using fluorescent lamp placed at a distance of 75 cm. On the other hand, the other PVC sheets were irradiated UV-ray using UV germicidal lamp placed at distance of 60 cm (UV intensity: 52.5 $\mu W/cm^2$) in clean-bench. These PVC sheets were irradiated for 1 week, 2 weeks, 1 month, 2 months or 3 months. After irradiation, the samples were stored in the shade. The positive control for visible light irradiation was a PVC sheet exposed to sunlight for approximately 1 year. The positive control for UV irradiation was a PVC sheet irradiated with a 254-nm UV lamp at a distance of 3 cm for 25 days. PVC tubing cut to a length of 10 cm was irradiated with a 254-nm UV lamp at a distance of 3 cm for 14 days.

2.3. GC–MS

A Hewlett-Packard HP 6890 Series GC system equipped with an auto-injector (Agilent Technologies, Palo Alto, CA) and a JMS700 spectrometer (JEOL, Tokyo, Japan) were used for gas chromatography-mass spectrometry (GC–MS). Chromatographic separations were performed with a BPX-5 fused silica capillary column (25 m × 0.22 mm i.d., film thickness: 0.25 μm, SGE Japan, Kanagawa, Japan).

A sample (2 μl) was injected in the pulsed splitless mode. The injector temperature was 260 °C. Helium was used as the carrier gas at a flow rate of 1 ml/min. The column temperature was programmed from 120 to 300 °C (held for 2 min) at a rate of 10 °C/min. The electron impact (EI)-mass spectrum was recorded at 70 eV for qualitative analysis, and ions of *m/z* 149.024 (DEHP) and 153.049 (DEHP-d_4) were selected as quantitative ions in selective ion monitoring (SIM) analysis (resolution = 5000) using the lock and check method of calibrating standard ions (*m/z* 168.989 of PFK). Quantitative analysis of each sample was repeated five times for calibration curves and twice for the other samples. The preparation of calibration curves and the calculation of quantitative data were performed using computer software TOCO, version 2.0 (total optimization of chemical operations), applying the function of mutual information (FUMI) theory (Hayashi and Matsuda, 1994; Hayashi et al., 1996, 2002; Haishima et al., 2001).

2.4. Migration test

The migration of DEHP from PVC sheets was examined in 5 ml of Sandimmun® prepared according to the instructions on the package insert. PVC sheets, which were irradiated or heat-treated were kept in test tubes and extraction was carried out by shaking at room temperature for 1 h. A 0.1 ml aliquot of the extract was pipetted into another test tube, and 2 ml of distilled water and 5 ml of diethyl ether containing 50 ng/ml DEHP-d_4 were added. The mixture was then subjected to extraction with shaking for 10 min. After centrifugation at 3000 rpm for 10 min, the organic phase was collected and dehydrated with anhydrous sodium sulfate, and subjected to GC–MS analysis.

PVC tubing cut to 10 cm length was used in the DEHP migration test, and filled with Sandimmun® (tube length, 8 cm; capacity, 0.285 cm^3; and surface area, 5.35 cm^2). The tubing was subjected to extraction with shaking at room temperature for 1 h. The extract was transferred into another test tube and treated in the same manner as that for PVC sheets.

2.5. Determination of DEHP compounds in PVC sheet by GC–MS

A PVC sheet sample (0.02 g) was dissolved in 20 ml of THF by soaking overnight at room temperature. A 0.1 ml aliquot of the solution was pipetted out and diluted with 2.0 ml of diethyl ether. A 0.1 ml aliquot was obtained, mixed with 50 ng/ml DEHP-d_4 (1 ml) and diethyl ether (8.9 ml), and then analyzed by GC–MS.

2.6. Analysis of surface structure

2.6.1. Infrared spectrometry

A JIR-SPX 200 (JEOL, Tokyo, Japan) was used for FT-IR spectroscopy coupled with attenuated total reflection (ATR) analysis. To analyze the PVC sheets, we used a germanium crystal, and the incidence angle was set at 45°.

2.6.2. Electron spectroscopy for chemical analysis

ESCA measurements were performed using an ESCA-3200 (Shimadzu, Kyoto, Japan). Only the inner side of the blood bag was measured for the heat treatment group and the visible light irradiation group, whereas both sides of the blood bag were measured for the UV irradiation group.

2.6.3. Static angle of contact

A solution of Sandimmun®, prepared according to the instructions on the package insert, was added dropwise to PVC sheets. After 120 s, the width and height of the droplet were measured with a G-1-1000 (ERMA, Tokyo, Japan). The static angle of contact with Sandimmun® was computed as follows:

$$L^2 = \left(\frac{w}{2}\right)^2 + (L-h)^2$$

$$\sin\delta = \left(\frac{w/2}{L}\right)$$

L is radius of droplet (mm); w is width of droplet (mm); h is height of droplet (mm); and (δ) static angle of contact.

Only the inner side of the blood bag was measured for the heat treatment group and the visible light irradiation group, whereas both sides of the blood bag were measured for the UV irradiation group.

2.7. Tensile test

A PVC sheet (0.7 cm × 3 cm, center width: 0.4 cm, thickness: 0.04 cm) was used as the sample (Fig. 1). Measurements were performed using an Autograph AG-20 kNG (Shimadzu, Kyoto, Japan) at a speed of 40 mm/min.

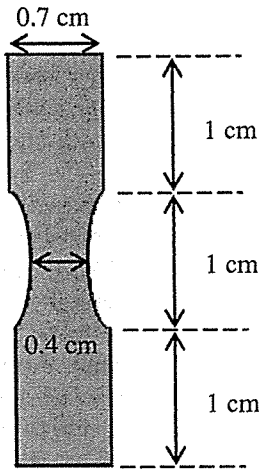

Fig. 1. The PVC sheet used in the tensile test A PVC sheet: 0.7 × 3 cm, center width: 0.4 cm, thickness: 0.04 cm.

3. Results and discussion

3.1. Determination of DEHP released from PVC products by GC–MS

First, the background was analyzed in order to examine the accuracy of the GC–MS method. When 50 ng/ml DEHP-d_4 with diethyl ether solution was used as the internal standard, 0.93 ± 0.31 ng/ml DEHP ($n = 5$) was detected in the internal standard. The DEHP background peaks in the internal standard solution were trace levels (S_0). In addition, the precision (SD) was expressed as SD_0. The limit of detection (LOD) and the limit of quantification (LOQ) of DEHP were calculated using S_0 and SD_0; LOD ($S_0 + 3 \times SD_0$) and LOQ ($S_0 + 10 \times SD_0$) were 1.9 and 4.0 ng/ml, respectively. A calibration curve was obtained for the peak ratio of DEHP to DEHP-d_4 versus the DEHP concentration level. The response was found to be linear in the validated range with a correlation coefficient (r) exceeding 0.999. Furthermore, the 95% confidence interval calculated by TOCO was sufficiently narrow to determine the amount of DEHP released from the PVC products. We found that this GC–MS method could be used for DEHP analysis with high accuracy.

The levels of DEHP that migrated from the PVC sheets were then determined, and the time course is shown in Fig. 2. Heat treatment and optical irradiation were each performed for 1 week, 2 weeks, 1 month, 2 months, and 3 months. At 2 months, the levels of DEHP migrating into Sandimmun® were slightly decreased by heat treatment and visible light irradiation, however no remarkable change was observed between the treatments, or between those treatments and their respective positive controls. The level of DEHP migration from the heat-treated PVC sheets has decreased the temperature-dependent. The most possible factor for the temperature-dependent, the sublimation/vaporization was occurred by heat treatment in PVC sheet. On the other hand, the significant change on

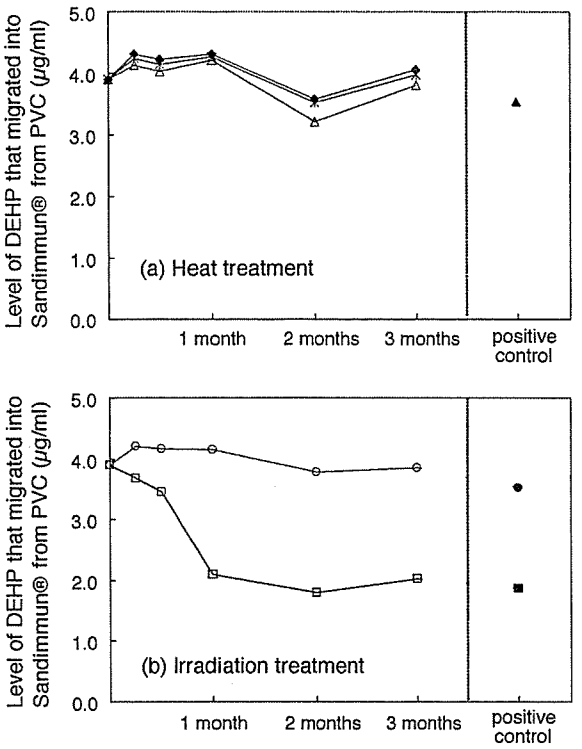

Fig. 2. Level of DEHP migrating into Sandimmun® injection from PVC sheet samples. (a) Heat treatment: PVC sheets were kept at 4 °C (♦); 37 °C (*) and 60 °C (△). Heated positive control: PVC sheets were kept at 100 °C for 25 days (▲). (b) Irradiation treatment: PVC sheets were irradiated with visible light (○) and UV (□). The visible irradiated positive control (●) was irradiated with sunlight for approximately 1 year. The UV-irradiated positive control (■) was irradiated with a UV lamp at 254 nm (3 cm, 25 days). The quantitative data were performed using computer software TOCO, Version 2.0 (Total Optimization of Chemical Operations), applying the function of mutual information (FUMI) theory.

migration was observed in UV-irradiated PVC sheets. The levels of DEHP migrating from the PVC sheets showed a time-dependent decrease in the UV irradiation group. At 1 month after UV irradiation, the level of DEHP migrating from the PVC sheet was reduced to approximately half that of the negative control. No significant change was observed thereafter, even if irradiation was continued. In addition, the level of DEHP migrating from the PVC sheet after UV irradiation over 3 months was not different from that of the positive control. We hypothesized that the reduction by half of the DEHP level has caused by UV-irradiated sides. We thought the UV-irradiated side (outer surface) of PVC sheet induces suppression in DEHP migration, and inner surface of PVC sheet dose not influence in migration. In order to confirm this hypothesis, we examined the PVC tubing that was able to distinguish outer and inner surface. The outer surface of the PVC tubing was subjected to strong UV irradiation. Subsequently, the level of DEHP migrating from the inner surface of the PVC tubing was determined. As a result, it was found that the level of DEHP released from the inner surface of the PVC tubing was almost the same as that of the negative control PVC tubing. It was concluded that the inner surface of the PVC tubing was not influenced by UV irradiation from the outside, since there was no change in the levels of DEHP released when compared with the control.

3.2. DEHP content examination

The DEHP content in the PVC sheets subjected to heat treatment or optical irradiation was determined. No significant difference in the DEHP content was found between the heat treatment groups and the visible light irradiation group. The positive controls of the two groups had almost the same DEHP content. On the other hand, the DEHP content in the UV-irradiated PVC sheets decreased slightly with time (Table 1). The most possible factor for the time-dependent, the sublimation/vaporization was occurred by UV-irradiated PVC sheet.

The rate of decrease in the DEHP content of the UV-irradiated PVC sheet was not equivalent to that of the level of migration. Therefore, the level of the suppression of DEHP migration was more remarkable than that of decreasing-content of DEHP.

3.3. Surface analysis

3.3.1. Surface analysis by FT-IR

FT-IR with ATR spectra was obtained from PVC sheets subjected to optical irradiation or heat treatment. Fig. 3a shows a characteristic absorption band at 635 cm^{-1}, due to C–Cl stretching vibration from PVC. We also observed absorption due to C–H from the aromatic compound and the carbonyl group from DEHP at 742 and 1720 cm^{-1}, respectively. Furthermore, an absorption band due to the alkane C–H bond from PVC and DEHP was found at nearly 1250 cm^{-1}. The FT-IR spectra of the heated-treated and visible

Table 1
DEHP content in PVC sheet samples (w/w, %)

	4 °C	37 °C	60 °C	Visible light	UV light
1 week	31.2 ± 0.09	31.9 ± 0.61	33.2 ± 0.35	34.1 ± 1.65	36.2 ± 2.14
2 weeks	32.6 ± 0.44	33.3 ± 0.25	31.7 ± 0.03	34.8 ± 1.36	34.7 ± 3.32
1 month	32.9 ± 0.39	34.2 ± 0.45	35.0 ± 1.11	34.1 ± 0.85	33.7 ± 5.11
2 months	33.2 ± 0.12	33.9 ± 0.25	33.3 ± 0.43	32.8 ± 0.18	29.4 ± 0.63
3 months	33.8 ± 0.04	32.9 ± 0.26	30.9 ± 0.34	29.5 ± 4.05	27.1 ± 0.37

Negative control samples: 36.0 ± 2.60%; positive control samples subjected to heat treatment: 32.4 ± 0.45%; positive control samples irradiated with visible light: 32.6 ± 0.70%; positive control samples irradiated with UV: 30.8 ± 0.53%.

light-irradiated PVC sheets were almost the same as that of the negative control. The spectrum was rectified using software because the ATR spectrum depended on the wavelength to calculate the areas of the characteristic absorption bands for DEHP or PVC. When the area ratios for the heat-treated or visible light-irradiated PVC sheets were compared with those of the negative control, no clear change was seen. On the other hand, as shown in Fig. 3b–f, the UV-irradiated PVC sheets were found to exhibit broadened absorption bands with time. These results led us to hypothesize that UV irradiation caused a change in the surface structure. The FT-IR spectrum of the non-UV-irradiated side was the same as that of the negative control, indicating that there was no change in the surface structure.

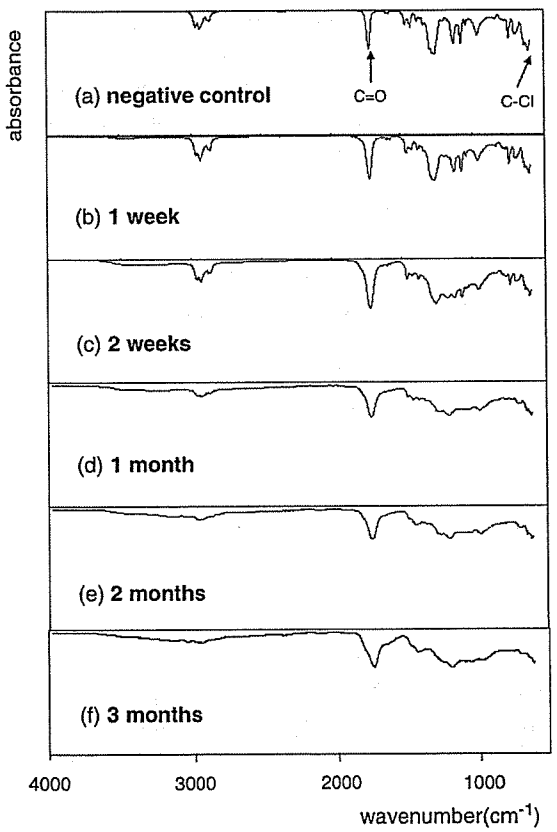

Fig. 3. FT-IR spectra of UV-irradiated and negative control PVC sheets FT-IR spectra of PVC sheets: negative control (a); and those irradiated with UV light for 1 week (b); 2 weeks (c); 1 month (d); 2 months (e) and 3 months (f).

3.3.2. *Surface analysis by ESCA*

Surface analysis of the PVC sheets was carried out and carbon, oxygen, chlorine and silicon were found on the sheet surface. As shown in Fig. 4a, the surface structure of the PVC sheets was not influenced by heat treatment or visible light irradiation because the composition ratio was maintained. On the other hand, in the UV-irradiated PVC sheets (Fig. 4b), the chlorine content was decreased and the oxygen content was increased with time. For the inner surface of the UV-irradiated PVC sheets, the composition ratio was hardly changed compared to the negative control in the period of 1 week to 1 month. However, after 2 months, the composition ratio was not changed at all compared with the negative control.

3.3.3. *Surface analysis by static angle of contact measurement*

In order to evaluate the affinity of the PVC sheets and the actual concentration of the Sandimmun® injection, we measured the static angle of contact. The static angle of contact was 37.1 ± 0.84 and 53.4 ± 0.93° for the outer and inner surfaces of the non-treated PVC sheets, respectively. We hypothesize that the differ-